Carbon balance and tree growth in a Fagus sylvatica stand

Stéphanie Lebaube, Noël Le Goff, Jean Marc Ottorini, André A. Granier

To cite this version:

Stéphanie Lebaube, Noël Le Goff, Jean Marc Ottorini, André A. Granier. Carbon balance and tree growth in a Fagus sylvatica stand. Annals of Forest Science, 2000, 57, pp.49-61. 10.1051/forest:2000100 . hal-02697143

Ann. For. Sci. 57 (2000) 49–61

Original article

Carbon balance and tree growth in a *Fagus sylvatica* stand

Stéphanie Lebaube[a], Noël Le Goff[b], Jean-Marc Ottorini[b] and André Granier[a,*]

[a] INRA Unité d'Écophysiologie Forestière, F-54280 Champenoux, France
[b] INRA Équipe de Croissance et Production, F-54280 Champenoux, France

(Received 7 December 1998; accepted 25 October 1999)

Abstract – The objectives of this study were 1) to scale photosynthesis from leaf to crown and to tree scale, 2) to determine the proportion of assimilated carbon used for wood construction and whether the fraction of assimilation used for production varies among social classes and 3) to validate the approach by comparing assimilation estimates with independent measurements provided by the eddy covariance technique (*EC*). Measurements (growth and gas exchange) were performed in a 30-year-old *Fagus sylvatica* stand during the 1997 growing season on five sample trees of different crown classes (dominant, codominant and intermediate trees). A nonlinear relationship between net CO_2 assimilation and photosynthetically active radiation (*PAR*) was found for each sample trees. Canopy net CO_2 assimilation was then modelled over a period of non limiting soil water soil water content. Simulated gross assimilation scaled to stand level was in good agreement with stand measurements performed by *EC*.

growth / carbon balance / photosynthesis / crown class / *Fagus sylvatica* L

Résumé – **Bilan de carbone et croissance dans un jeune peuplement de *Fagus sylvatica*.** Les objectifs de cette étude étaient 1) d'estimer la photosynthèse à l'échelle de la couronne, puis à l'échelle de l'arbre à partir de mesures foliaires, 2) de déterminer la proportion du carbone assimilé utilisée pour la construction de bois et sa variation en fonction du statut social de l'arbre, 3) de valider l'estimation de l'assimilation en la comparant à une mesure indépendante (technique des corrélations turbulentes, *EC*). Les mesures (croissance et échanges gazeux) ont été effectuées pendant la saison de végétation 1997 sur cinq hêtres de 30 ans de statuts sociaux différents (dominant, codominant et dominé). Une relation non linéaire entre l'assimilation nette de CO_2 et le rayonnement photosynthetiquement actif (*PAR*) a été établie pour chaque arbre échantillon. L'assimilation nette de CO_2 à l'échelle de la couronne a ensuite été estimée pour une période sans stress hydrique. L'estimation de l'assimilation brute à l'échelle du peuplement à partir de mesures foliaires est en bon accord avec des mesures effectuées à l'échelle du peuplement par *EC*.

croissance / bilan de carbone / photosynthèse / statut social / *Fagus sylvatica* L

1. INTRODUCTION

Understanding of the elementary processes and biochemistry of photosynthesis was improved during the last two decades [21]. Carbon assimilation has been studied on cellular, leaf and plant levels [7]. Responses at leaf level to short-term changes in environmental factors (light, temperature, CO_2) is well known. Less is known about responses of whole tree and of forest ecosystems [45]. On the other hand, linking gross or net assimilation to tree growth in order to estimate stand productivity needs more investigations [24]. Even if there is no obvious relationship between photosynthesis and wood production [14], stand productivity is

---

* Correspondence and reprints
Tel. (33) 03 83 39 40 41; Fax. (33) 03 83 39 40 69; e-mail: agranier@nancy.inra.fr

limited by canopy photosynthesis, which sets its upper limit. The increase of biomass depends on the net primary productivity (*NPP*).

To predict effects of global environmental change on ecosystems and influence of forests on carbon and water cycles, models of canopy and ecosystem processes are essential tools. Models of canopy photosynthesis of both multilayer and “big leaf” types exist. The first one integrates fluxes for each layer to obtain the total flux [37]. Alternative to the multilayer models has been presented [16] by separating sunlit and shaded leaf fractions of the canopy based on radiation penetration. The big leaf model applies properties of the whole canopy to a single leaf [3, 39, 46]. Our approach consists of an intermediate one and is based on experimental relationships obtained *in situ* over one growing season. As in many of studies, assimilation of trees was studied at leaf scale. The description and parameterisations of the leaf processes at both spatial and temporal scales enable to extend our work to larger scales (tree and stand). This kind of model is commonly referred as “bottom up model” [5, 41].

The aim of our study was 1) to scale photosynthesis from leaf to crown level and to tree scale, 2) to determine the proportion of assimilated carbon used for wood construction and whether the fraction of assimilation used for production varies among social classes and 3) to validate the approach by comparing assimilation estimates with independent measurements performed by the eddy covariance technique (*EC*) which provides a method to assess the total carbon exchange rate at the ecosystem scale [26].

2. MATERIALS AND METHODS

2.1. Site

The field site is located at Hesse, France (lat. 48°40' N, long. 7°05', 300 m above mean sea level) in a 30-year-old naturally regenerated beech stand. The size of the sample area is 0.6 ha. It is an almost pure stand of beech (*Fagus sylvatica* L.). Soil is a gleyic luvisol according to F.A.O. classification. The pH of the top soil (0–30 cm) is 4.9 with a *C/N* ratio of 12.2 and an apparent density of 0.85 kg dm^{-3} and is covered with a mull type humus [19]. Clay content ranged between 25% and 35% within 0–100 cm depth, and was about 40% below 100 cm. The main characteristics of the site in 1997, including climate, are shown in *table I*.

Table I. Main climatic and vegetation characteristics of the Hesse site. Biometric data correspond to the year 1997.

Mean tree height	12.7 m
Mean circumference at 1.3 m	22.7 cm
Basal area	20.7 m^2 ha^{-1}
Tree density	~ 4000 trees ha^{-1}
Age	25 to 35 years
Mean air temperature	9.2 °C
Mean annual precipitation	820 mm

2.2. Measurements at the stand level

Measurements of carbon dioxide, water and energy fluxes were made above the stand. A set of micrometeorological instruments was suspended 18 m above the ground (3 m above the tallest trees) on a walk-up scaffold tower provided by the EUROFLUX project. The eddy covariance technique allowed measuring CO_2 and water vapour flux densities between the forest and the atmosphere [15]. Wind velocity fluctuations were measured with a three-dimensional sonic anemometer (Solent R2, Gill Instruments Ltd., Lymington, UK). Carbon dioxide and water vapour fluctuations were measured with an infrared gas analyser (Licor LI-6262, Lincoln, Nebraska USA). Data were digitised ten times per second; real time processing of fluxes was done using the Edisol software (University of Edimbourgh, UK). Using the convention adopted by atmospheric scientists, positive mass and energy flux densities represent transfer from the surface to the atmosphere; negative values denote the reverse. Climate data were monitored above the canopy and logged every 30 min with a Campbell CR7 data logger (UK). A weather station included a pyranometer (Cimel, France), a net radiometer (REBS, Seattle, USA), a ventilated psychrometer with Pt-100 platinum sensors (model INRA) and an anemometer (Vector Instruments, Rhyl, UK). Soil temperature was measured with thermocouple probes, spaced at 0.05, 0.10, 0.20, 0.40 and 0.80 m below the soil surface.

Circumference increment at breast height was measured manually every two weeks on a sample of 541 trees of the experimental plot from March to October 1997. The reference level was marked on the bark to increase accuracy of measurements. Four circumference classes were considered (<200, 200–300, 300–400, >400 mm). These classes corresponded to trees in suppressed, intermediate, codominant and dominant crown position in the canopy.

2.3. Measurements at the whole-tree level

Our sampling scheme was based on five trees surrounding one of the scaffold towers: trees of almost all crown classes were represented in the sample (2 dominant, 1 codominant and 2 intermediate trees). Trees were classified according to the criteria of Kraft [30]. See characteristics of the 5 sample trees in *table II*.

Details on the measurements performed on the sample trees during the growing season 1997 are described in *table III*.

Photosynthetically active radiation (*PAR*) was measured at two heights in the crowns of the 5 sample trees using 30 cm long linear *PAR* sensors attached to the branches where net assimilation measurements were performed. Those *PAR* sensors were constructed with 20 silicon cells (Solems. France) by P Gross.

2.4. Allometric relationships

Trees analysed for biomass evaluation were sampled in two successive years: 1996 and 1997, in late September. Tree inventory of Hesse experimental stand was made in 1996, prior to the growth period, and a frequency distribution of girth at 1.30 m, was obtained. Examination of trees of each crown class (dominant, codominant, intermediate, and suppressed trees) allowed an estimation of the girths corresponding to the lower bounds of the dominant, codominant, and intermediate tree classes. These bounds revealed that the proportional sampling of each crown class approximately yielded the same number of trees in each of the four classes. Following this sampling scheme, 11 trees were sampled the first year, and 12 trees the second one, equally distributed in each crown class. More details can be found in [25].

2.5. Bud-burst observations

Bud-burst observations were recorded from mid-March to end of May on the sample of five trees on a 3-day time notation (*table III*). Bud development was described according to a six stage scale (dormant winter buds, swollen buds, broken buds, just-unfolded leaves,

Table II. Mean tree characteristics in 1997.

Sample trees	101	32	27	31	A
Circumference at 1 m 80 (cm)	41.5	35.5	31.7	20.2	23.5
Height (m)	15.0	15.5	13.9	12.5	13.7
Crown class	dominant	dominant	codominant	intermediate	intermediate
Above-ground biomass (kg)[1]	88.8	53.6	45.3	13.6	19.7
Stem biomass (kg)[1]	73.2	45.3	38.6	12.1	17.3
Root biomass (kg)[1]	16.5	9.8	8.2	2.3	3.5
Total leaf area (m^2)[1]	37.7	24.6	21.4	8.6	11.1
% of sun leaf area[1]	55	46	43	21	28

[1] Estimated from relationships established by Le Goff and Ottorini (unpublished data).

Table III. Measurements performed during 1997.

Measurements	Instrumentation	Frequency	Sampling
Microclimate	weather station	average every 30 min	3 m above the stand
Radiation (PAR)	linear sensors SOLEMS	average every 30 min	5 trees * 2 crown levels (bottom and top)
Bud burst		3 days (from 15/03 to 31/05)	5 trees
LAI	DEMON	2 times at (8h, 10h, 12h)	5 to 7 replicates (at stand level)
Predawn Leaf Water potential	Scholander chamber	14 to 30 days	5 trees * 1 canopy level * 2 leaves
Radial growth	dendrom. bands	3 times per week	5 trees * 3 stem heights
Carbon uptake	Li-Cor 6200	14 to 30 days	5 trees * 2 canopy levels * 2 branches (4 leaves)

unfolded leaves, developed leaves with elongation of twigs) [38]. Bud-burst index ranged from 0 to 100 and was computed as the mean notation.

2.6. Leaf area index

Leaf area index was measured with a DEMON leaf area analyser (CSIRO, Canberra, ACT, Australia) [11, 34] two times during the growing season (*table III*). Leaf litter was collected in 42 sampling traps periodically emptied to avoid decomposition, during leaf fall in October and November. In the laboratory, projected leaf area was determined using a Delta-*T* Image analyser system (ΔT Area Meter, ΔT Devices, Cambridge, UK) after drying.

2.7. Radial increment

Seasonal circumference increment at the height of 1.30, 6.50 and about 10.00 m was measured using dendrometer bands on the five sample trees (*table III*) from May to October 1997.

2.8. Net CO_2 assimilation

Carbon dioxide uptake was measured on fully expanded foliage on the 5 sample trees (*table III*). Net CO_2 assimilation (A_n) was measured *in situ* with a closed, battery-operated portable LI-6200 photosynthesis system (Li-Cor, Inc., Lincoln, NE) and expressed on a leaf area basis. We measured the diurnal course of leaf CO_2 exchange under ambient conditions. Twenty branches were chosen for gas exchange measurements (four on each tree: two for one canopy position at each tree). Each sample was composed of about four leaves. The same leaves were measured throughout the growing season. Gas exchange was calculated using the total leaf area within the cuvette.

During the period June-September 1997, the diurnal course of leaf CO_2 exchange was monitored twice a month for each sample. One diurnal course consisted in twenty measurements (5 trees × 2 levels × 2 branches) repeated every 2h from approximately 8:00 to 16:00 TU.

2.9. Tree carbon increment

We estimated an annual growth budget for each tree by measured or estimated biomass (foliage, fine roots, bark and coarse roots, branches, stems). Stem biomass increment was calculated from the continuous circumference measurements (dendrometer bands). Foliage, roots (except fine roots which could not be measured), bark, and branch biomass were estimated using allometric relationships with circumference at breast height. Annual growth for each component was calculated as the difference between biomass at the beginning and end of the year. Those data were converted in carbon mass, using wood density of the different tree compartments (unpublished data) and the following correspondence: 1 kg of dry matter =0.437 kg of carbon in stems and roots, =0.442 kg in branches, =0.457 kg in leaves [44].

Allometric relationships were used to estimate annual increment (I) for each tree component in kg of dry matter and leaf area (LA) in m^2:

$$I_{stem}{}^{0.2} = -2.2155 + 1.7656 * C_{130}{}^{0.2} \qquad r^2 = 0.93 \qquad (1)$$

$$I_{branch}{}^{0.2} = -1.6658 + 1.2984 * C_{130}{}^{0.2} \qquad r^2 = 0.95 \qquad (2)$$

$$\ln_{root} = -11.2318 + 3.0579 * \ln C_{130} \qquad r^2 = 0.99 \qquad (3)$$

$$\ln LA = -3.2627 + 1.8307 * \ln C_{130} \qquad r^2 = 0.92 \qquad (4)$$

where C_{130}: circumference at breast height.

2.10. Annual carbon balance at tree scale

Carbon balance was estimated over the period from *DOY* (Day Of Year) 120 to 260.

2.10.1. Assimilation

Over four hundred data relating CO_2 flux in the canopy to simultaneously recorded *PAR* have been compiled. We did not evidence dependency of net assimilation to other factors than *PAR*. Measurements of net assimilation were fitted on *PAR* for each level of the canopy and each tree using non linear functions calibrated on field data, of the following type:

$$A_n = \frac{a + b * PAR - \left[\left(a + b * PAR\right)^2 - 4 * a * b * c * PAR\right]^{1/2}}{2 * c} \qquad (5)$$

where *a*, *b*, *c*, *d*: fitting coefficients; *c* (concavity) was set to 0.7

In a second step, instantaneous net assimilation was calculated using equation (5) and continuous *PAR* measurements in the crowns (5 trees × 2 levels). Total net assimilation per tree was obtained by multiplying instantaneous values by leaf area of each half crown and summing values of the 2 half crowns. As we did not measure A_n during the phase of rapid leaf expansion, we assumed

A_n to have increased linearly between *DOY* 120 and 150 as confirmed by eddy covariance measurements at stand level.

2.10.2. Respiration

Ecosystem respiration (R_{eco}) was measured over the stand by *EC* during the night and extrapolated over the entire day. R_{eco} increased with soil temperature measured at a depth of 5 cm (T_{soil}) [25]. CO_2 efflux at the soil surface (R_{soil}) was estimated from periodic cuvette measurements scaled to the stand and described as a function of soil temperature (T_{soil}) [19]. Aerial biomass respiration (R_{bio}) was calculated as the difference between ecosystem respiration and CO_2 efflux at the soil surface:

$$R_{eco} = 0.542 * 10^{0.0559 * T_{soil}} \quad (6)$$

$$R_{soil} = 0.436 * 10^{0.0509 * T_{soil}} \quad (7)$$

$$R_{bio} = R_{eco} - R_{soil}. \quad (8)$$

These stand-level respiration terms were scaled down at the tree level, assuming that tree aerial biomass respiration and root respiration were proportional to aerial biomass and root biomass, respectively. Therefore, we estimated aerial biomass respiration and root respiration for each sampled tree, using respectively their aerial biomass and root biomass (calculated from circumference at breast height as explained previously).

Leaf respiration was assumed to be equal to half the aerial biomass respiration (R_{bio}). Diurnal leaf respiration (R_{ld}) was assumed to be equal to night respiration. Root respiration was estimated as 56% of the total soil efflux [20].

$$R_{ld} = 0.25 * R_{bio} \quad (9)$$

$$R_{root} = 0.56 * R_{soil}. \quad (10)$$

2.11. Validation at stand scale

For validation, measurements of net assimilation performed at leaf level were scaled to tree and to stand levels. Net assimilation at the stand scale (A_n) was obtained after multiplying net assimilation of individual trees (expressed per unit of leaf area) by the LAI corresponding to each crown class (2.6, 1.6 and 1.5 $m^2\ m^{-2}$ in dominant, codominant and intermediate+suppressed trees, respectively). Then, we compared scaled chamber measurements of gross assimilation (GEP_{SL}) with ecosystem gross assimilation (GEP_{EC}) calculated by adding ecosystem respiration to net ecosystem flux measurements (NEE_{EC}) (expressed as an absolute value):

$$GEP_{SL} = A_N + R_{ld} \quad (11)$$

$$GEP_{EC} = NEE_{EC} + R_{eco}. \quad (12)$$

2.12. Statistical analysis

Growth, photosynthesis and carbon balance were analysed with the General Linear Models procedure (Statistical Analysis Systems Institute 1988). An ANOVA was used to test differences between crown classes and between levels in the canopy (*table IV*).

3. RESULTS

3.1. Bud-burst index and leaf area index

Seasonal time courses of circumference showed that radial increment started by the *DOY* 120 (*figure 1*). At this time, transpiration has just begun to be detectable, as indicated by sap-flow measurements, and bud-burst index was about 80% (*figure 2*). Leaf biomass and leaf area were supposed to increase linearly during the period from budbreak (*DOY* 120) to the peak of leaf index area occurring by the *DOY* 152 (*LAI* of 5.7).

3.2. Radial increment

Cumulated radial increment differed significantly among social status (*table IV*). Radial increment of intermediate trees was too low to be measured accurately with dendrometer bands. The seasonal pattern (*figure 1*) displayed a rapid increase of radial increment in spring from *DOY* 120 to mid-July, followed by a slow decrease later. Radial increment stopped by the end of august.

Comparing growth trend of the sample trees (at breast height) with radial increment at stand scale, we found a very good agreement between the two measurements and observed the same seasonal pattern.

Table IV. SAS results (Bonferroni T tests, alpha = 0.05).

Variables	Date (F1)	Level (F2)	Crown class (F3)	F2* F3
Radial growth	***	NS	***	***
Photosynthesis	***	***	***	***
PAR (radiation)	*	***	***	***

($p > 0.05$: N.S; $0.01 < p < 0.05$: *; $0.001 < p < 0.01$: **; $p < 0.001$: ***).

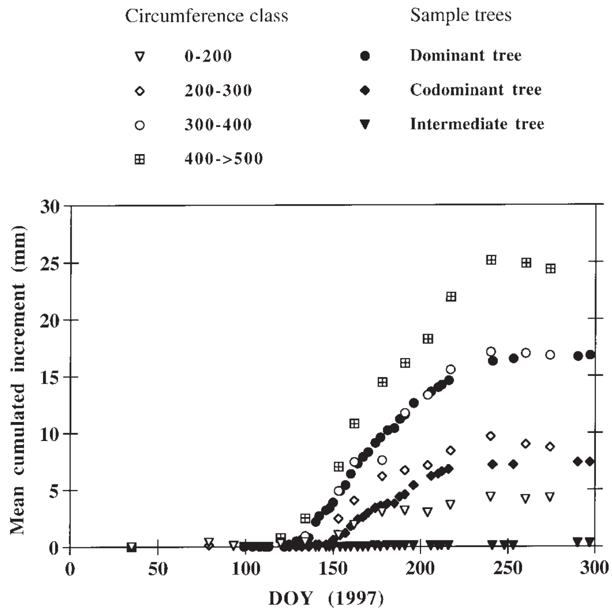

Figure 1. Seasonal time course of radial growth at breast height during the growing season 1997, at stand scale and on the 5 sample trees. Data were separated into four circumference classes (corresponding to different crown classes).

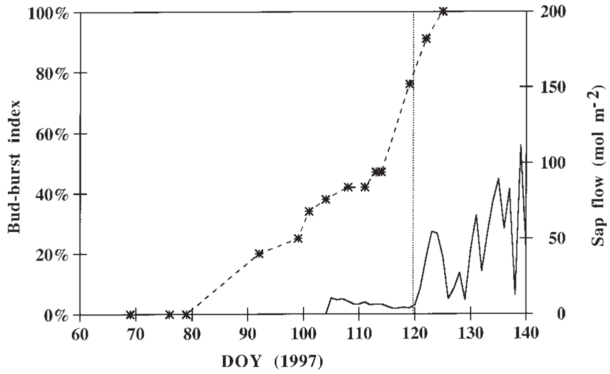

Figure 2. Variation of bud-burst index (asterisks) and sapflow (solid line) during the early period of 1997 growing season. The bud-burst index is ranged from 0 to 100. The threshold for the beginning of the growing season 1997 is shown and indicates the date (*DOY* 120) at which starts calculation for carbon balance.

3.3. Biomass distribution

The biomass of the main tree compartments was expressed as a proportion of the total tree biomass in *table V*. The leaf biomass/branch biomass ratio decreased with increasing tree size (*figure 3*).

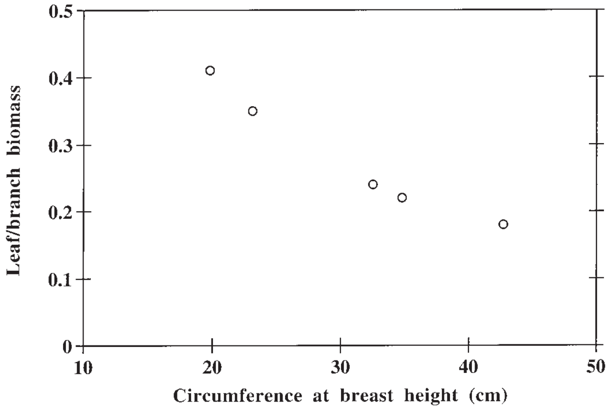

Figure 3. Leaf biomass/branch biomass ratio as a function of circumference at breast height.

3.4. Net assimilation

Representative examples of net assimilation functions of *PAR* are given in *figure 4* for one dominant tree and one intermediate tree. All the relationships show a rather large scatter of data (square-*r* ranged between 0.5 and 0.6) (*table VI*). This behaviour can be caused by several factors among which environmental factors. The achievement of a saturating maximum, especially for dominant trees, was not observed. CO_2 uptake differed significantly according to social status and to level within the crown (*table IV*). Carbon uptake was higher in dominant and codominant classes than in intermediate one and was higher at the top of the crown than at the bottom. Nevertheless, the difference was not significant among social status for the lowest position in the crown. It has to be stressed that we probably under-estimated

Table V. Relative biomass distribution in the tree compartments.

Caracteristic	101	32	27	31	A
Stem biomass (%)	70	71	72	76	75
Branch biomass (%)	13	11	10	7	8
Leaf biomass (%)	2	2	2	3	3
Above-ground biomass (%)	84	85	85	85	85
Root biomass (%)	16	15	15	15	15

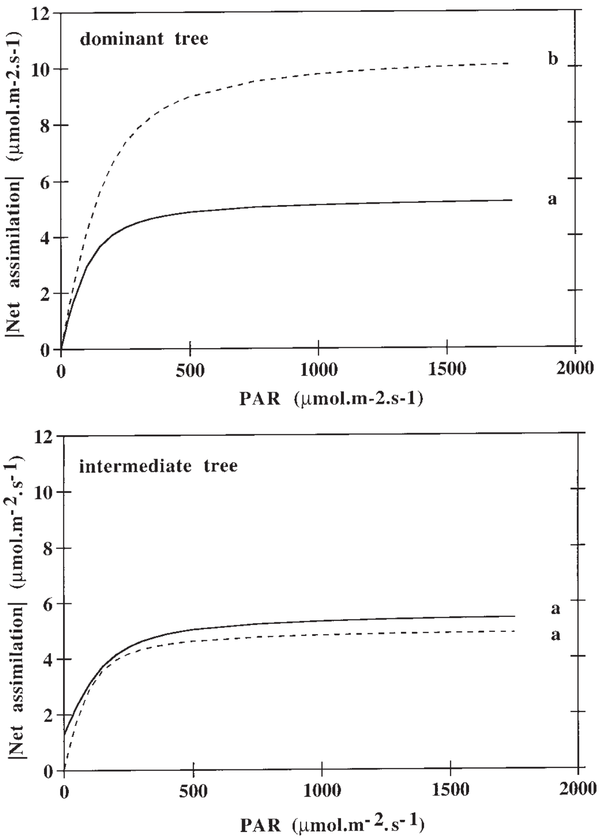

Figure 4. Representative examples of net assimilation as a function of photosynthetically active radiation for a dominant tree and an intermediate one. Data were collected in the upper level of the canopy (dotted line) and in the lowest level (plain line) and restricted after full-leaf expansion (*DOY* from 150 to 250). Function with the same letter were not significantly different. Note that net assimilation is expressed as an absolute value.

Table VI. Fitting coefficients used in equation (5).

Fitting coefficient	101 ul	32 ul	27 ul	31 ul	A ul
a	10.50	7.37	8.74	4.99	5.10
b	0.050	0.043	0.101	0.041	0.029
d (× 10^{-4})	1.23	9.70	27.00	194.00	9.32
square-*r*	0.668	0.628	0.682	0.534	0.558
Fitting coefficient	101 ll	32 ll	27 ll	31 ll	A ll
a	5.35	4.85	3.50	4.31	3.26
b	0.040	0.063	0.040	0.023	0.083
d (× 10^{-4})	10.00	1.85	10.00	12700.00	3.68
square-*r*	0.525	0.772	0.530	0.594	0.624

(ul: upper level of the canopy; ll: lower level of the canopy).

gross assimilation for tree No. 32, due to a bias in measurements (we observed that sample branches in the upper level of the crown were under shaded position during the afternoon).

3.5. Comparison of gross assimilation estimates

We compared the two estimates of daily gross assimilation at the stand level. The first one was derived from measurements on our 5-trees sample scaled to the stand. The other one derived from eddy covariance measurements. The comparison was done for daily variations (*figure 5*) and over the whole-growing season with daily-cumulated values (*figure 6*).

3.5.1. Daily variation

In *figure 5* a typical daily trend of gross assimilation estimated from scaled leaf and from *EC* measurements is presented. This graph represents *DOY* 190, under non limiting soil water supply (–0.45 MPa of predawn leaf water potential) and high irradiance. Assimilation peaked at about 12:00 hours (20 μmol m^{-2} s^{-1}) corresponding to maximum *PAR*. The CO_2 assimilation became negative at about 4:00 and reached zero at about 21:00. Both estimates of gross assimilation were in the same range and followed the same pattern, although a time shift was observed in the afternoon. This phenomenon was probably due to a bias in photosynthesis measurements done on leaves receiving higher radiation than the average canopy at that time. The decrease of assimilation noted in the afternoon is roughly proportional to the decrease of *PAR*. The fast variations of gross assimilation observed at 2:30 and 23:00 are probably due to measurements errors often observed with EC [8, 9].

3.5.2. Seasonal variation

Leaf measurements scaled to the stand (GEP_{SL}) were compared to measurements of GEP_{EC} at stand scale. The time course of both estimates during 1997 is shown in *figure 6*. The same seasonal patterns were observed: a rapid increase of carbon flux occurred in spring for about 30 days, maximum fixation rates being observed between *DOY* 150 to 190, and a slow decrease later. Over the whole vegetation period (*DOY* 120 to 260), cumulated GEP equalled to –1245 g C m^{-2} yr^{-1} and –1298 g C m^{-2} yr^{-1} for GEP_{EC} and GEP_{SL}, respectively. Gross assimilation courses from the two approaches were in good agreement (*figure 6*), except for some of the extreme values of gross assimilation from *EC* measurements. There was a tendency for scaled leaf estimates to be lower than *EC* measurements at the end of

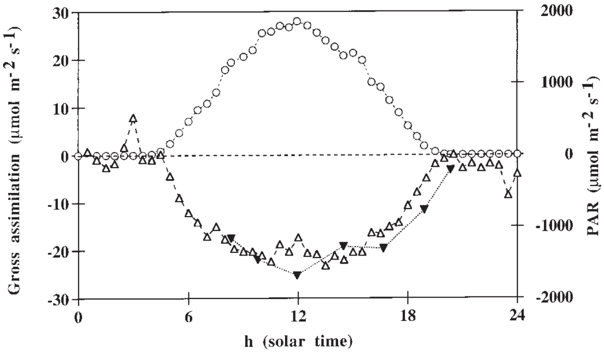

Figure 5. Diurnal pattern on *DOY* 190 of radiation and estimates of gross assimilation. The symbols represent the incoming photosynthetically active radiation (circles), gross assimilation calculated from eddy covariance measurements (triangles) and gross assimilation derived from measurements using Li-Cor 6200 on 5 trees scaled to the stand (inverted triangles). Data are averaged according to time of day.

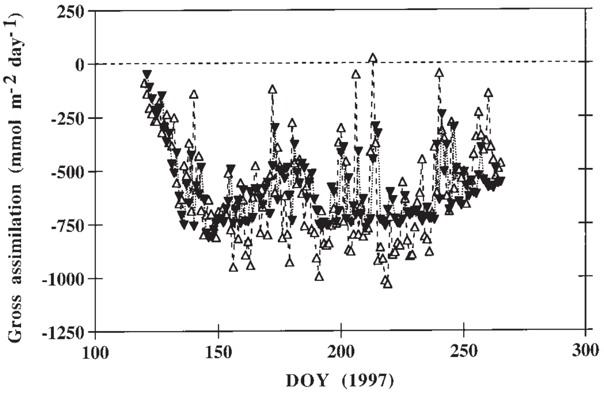

Figure 6. The day to day variation of the two estimates of gross assimilation (*GEP*) during the growing season 1997. The symbols represent eddy covariance measurements (triangles) and measurements using Li-Cor 6200 on 5 trees scaled to the stand (inverted triangles).

spring (*DOY* 140 to 150) and at the end of summer (*DOY* 240 to 270).

3.6. Carbon budget at the tree scale

Figure 7 shows the 3 major components of annual carbon fluxes for each sample tree: gross assimilation, aerial and belowground biomass respiration. Gross assimilation reached 11000 g C yr^{-1} for dominant tree; it was in the range 4000 to 6000 g C yr^{-1} for the codominant trees and between 1000 and 2000 g C yr^{-1} in the smallest trees. Such large differences in gross assimilation were due to differences: i) in leaf area, ii) in the amount of transmitted *PAR* per unit of leaf area which depends on the crown status, iii) in the response curves to *PAR*. Ratio of biomass respiration to gross assimilation increased from the dominant (c.a. 40%) to the intermediate crown classes (c.a. 60%).

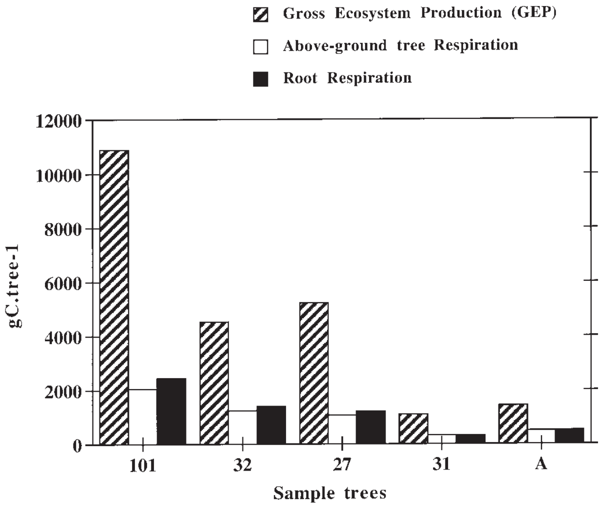

Figure 7. Annual carbon fluxes in each sample tree during the growing season 1997 (from *DOY* 150 to 266).

Annual carbon increment for each sample tree is presented in *figure 9*. Tree carbon increment was derived from dendrometer band measurements and estimates using allometric relationships. For intermediate trees, annual increment was estimated using allometric relationship (Eq. 1) as radial increment was not measured accurately with dendrometer bands. *Figure 8* shows that carbon in leaves represented a high proportion of annual carbon allocation (about 25%) in trees.

Annual carbon increment per tree is compared to tree carbon balance in *figure 9*. Both budgets (carbon fluxes *vs*. growth) were in the same range, except for trees No. 32 and No. A due respectively, to a bias in measurements (see before) and illness of tree No. A.

4. DISCUSSION

4.1. Bud-burst index and leaf index area

Radial increment increased as soon as leaf expansion began and CO_2 assimilation had started. In diffuse

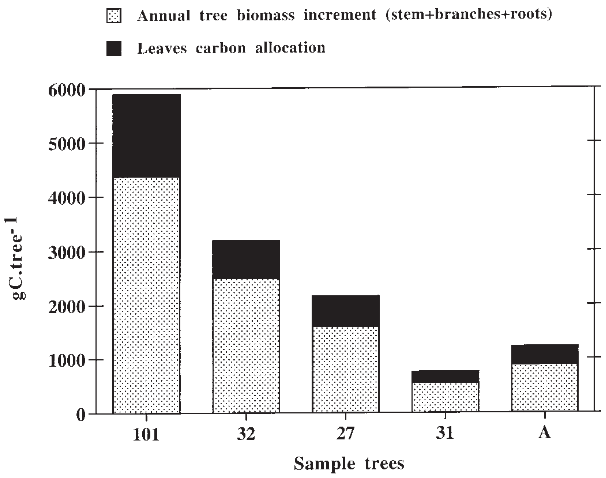

Figure 8. Annual biomass increment converted to carbon mass for each sample tree during the growing season 1997 (from *DOY* 150 to 266). Data distinguished carbon allocation between ligneous parts and leaf organs.

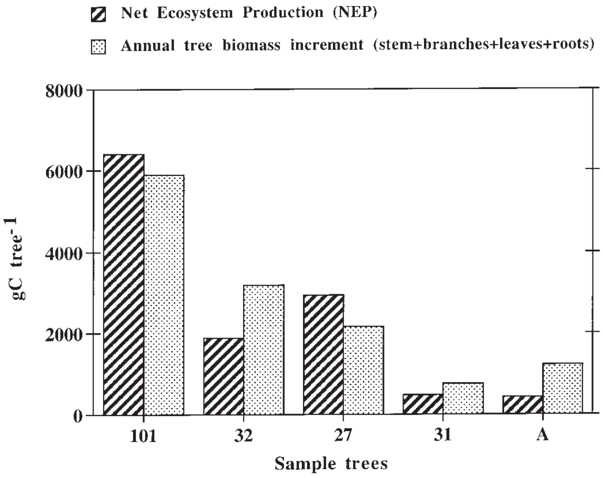

Figure 9. Comparison between net carbon fluxes and annual biomass increments converted in carbon mass for each sample tree during the growing season 1997 (from *DOY* 150 to 266).

porous species like beech, cambium re-activation and bud-burst occur simultaneously and growth follows bud-burst [31–33]. In contrast, the earlywood of ring-porous hardwood species like oak is formed from carbon resources accumulated during the previous years [12]. At the end of spring (June), the main part of the radial increment is achieved. Cambium re-activation preceding leaf development was observed by [27] and [52] and characterised ring-porous species.

4.2. Radial increment

Water availability was high during the growing season 1997, as indicated by the predawn water potential values (mean values –0.25 MPa) (unpublished data). So water availability was not a limiting factor for beech growth [35].

4.3. Biomass distribution

Stem represented about 70% of the total biomass. This value is consistent with values reported in *Fagus sylvatica* stands by Santa Regina et al. [44]. The stem is therefore the part of the tree that most contributes to the total biomass.

The contribution of leaf organs to total biomass was about 2%. This value is similar to values reported in literature [36, 44]. Although the contribution to the carbon stock is very low, leaf organs represent about 25% of the annual carbon allocation.

The branch fraction increased with increasing tree size and ranged from 8% to 13%. The values are less important than those reported by Santa Regina et al. [44] (21.9% in beech forest). But biomass distribution corresponds to pattern described in literature: dominant trees have a higher fraction of branch biomass than smaller trees, which means that dominance affects the amount of crown biomass [13]. Dominant trees invest more in the canopy and therefore are able to maintain a relatively large crown [10]. Furthermore, a decrease of *L*/*B* ratio as crown class increases was observed. This can be ascribed to crown expansion as more branches will be needed to increase crown size and as foliage is concentrated at the end of the branches (crown mantle) in order to optimise radiation interception [29].

4.4. Trends of CO_2 exchange

At daily scale, trends of gross assimilation from both means of estimations (from scaled leaf and from *EC* measurements) and especially maximum of gross assimilation were consistent with results reported in literature [50]. Beech as oak has photosynthetic capacities lower than major deciduous broad-leafed trees [14].

Differences of net assimilation between upper and lower levels in the canopy can be explained by a decrease in nitrogen concentration with depth in the canopy (usual pattern) in beech foliage [43] and by canopy shading effects [51] which involves light limitation of photosynthesis at the lowest level of the canopy.

During late summer, carbon fixation by the ecosystem decreased slowly (i.e. *NEE* increased towards 0), due to the combination of: 1) the seasonal decrease in incoming *PAR* that reduced beech photosynthesis, 2) soil water content decreased in the roots zone, as measured with neutron probe; the threshold *REW* = 0.4 corresponding to water stress onset was reached in 1997 on *DOY* 250 (7 September), 3) later, leaf yellowing and senescence (after *DOY* 260). Besides a direct effect of *PAR*, decrease of assimilation noted by the end of the growing season could be due to a decrease in nitrogen [6, 40], but we noticed no change in the relationships between net assimilation and *PAR* for each sample trees.

4.5. Pattern of carbon allocation

Stem and leaves represented respectively about 50% and 25% of the annual carbon allocation and can be considered as major carbon sinks. Within the plant, carbon allocation is regulated by source-sink interactions [17]. Moreover, carbon allocation to different sinks is largely independent of assimilate production, but is related to sink strength. Sink strength is related to size, growth rate, metabolic activity and respiration rate [22].

Intermediate and suppressed trees had mostly shaded branches. Their carbon production equals 20% of carbon production by large trees. Shaded branches contribute little carbohydrate to the rest of the tree and fix just enough carbon to meet their own needs [53]. They are considered as autonomous with respect to carbon i.e., these branches do not drain carbohydrates to the stem and roots [49]. Pattern of carbon allocation of intermediate and suppressed trees can be similar to the one just described.

4.6. Assumptions made

4.6.1. Growth

One of the aims of this work was to determine the proportion of assimilation used for wood construction. Annual biomass increment was therefore calculated as the difference in biomass of tree compartments at the beginning and the end of the year. We did not consider any turnover rates of various tree compartments. As on an annual basis, total growth includes physiological phenomena [53].

4.6.2. Assimilation

Our purpose was to monitor A_n under ambient environmental conditions in order to get an estimate of carbon budget at tree scale. Therefore, the functions used to estimate leaf seasonal photosynthesis are not true “light responses curves”, because factors other than light varied significantly during the daylong measurements (air temperature, ambient CO_2 concentration and VPD). However, it served well for the prediction of photosynthesis because it integrated changes in ambient microclimate that most likely accompany changes in irradiance. Witowski followed the same argument [53]. Moreover, daily fluxes of carbon exchange are well related to daily incident *PAR* [26].

No clear effect of air temperature was observed here, probably because it remained below the threshold of photosynthesis decrease.

When calculated from mean irradiance absorbed by the canopy, photosynthesis is overestimated [48]. Because light response of photosynthesis is non-linear, models have to discriminate between radiation absorbed by shaded and sunlit [48]. In the present study, we assumed the canopy could be the sum of only two layers. In our model, radiation was measured continuously nearby shaded and sunlit leaves in each canopy during the growing season.

4.6.3. Respiration

Ratio of biomass respiration to gross assimilation was consistent with range of annual costs of respiration given by Edwards et al. [18] and Ryan et al. [42] even if several assumptions have been made. In the carbon balance, there was no distinction between both types of respiration and their different substrates. Although it is generally recognised that respiration can be functionally separated into growth and maintenance respiration [2]. But there is no biochemical evidence to determine whether growth and maintenance respiration consumes only newly synthesised carbohydrates and storage substances, respectively [47].

The assumption that daylight leaf respiration equals night respiration is questionable, because dark respiration varies between night and daylight hours [4]. However, no quantitative information regarding a possible daylight increase at the stand level could be found.

We estimated respiration using a function of temperature as there is a strong dependence of respiration on temperature [23, 54]. We then made the assumption that respiration is proportional with the amount of biomass. Witowski already estimated respiration using the dependence of branch and needle respiration rates on temperature [53]. Ruimy et al. [41] noticed that in the light, maintenance and heterotrophic respiration rates followed the diurnal course of temperature. And for a given temperature, maintenance respiration rate depends principally on the biomass of the canopy. Moreover, efflux of CO_2 from foliage (dark respiration) and fine roots was found linearly related to biomass by Ryan et al. [43].

5. CONCLUSION

The leaf measurement reproduced most features of the diurnal and seasonal changes observed in the tower data and gave good overall agreement with measurements of stand gross assimilation. This behaviour was also noticed by Wofsy et al. [54] and Aber et al. [1]. The good agreement between predictions and measurements of overall canopy assimilation can be explained because most of the exchanges of mass and energy take place in the upper half of the canopy [28] and we are confident in the data sets observed in the upper level of the canopy.

Although this study was performed on few trees, it was a first approach to estimate tree NEP depending on the crown class and stand NEP, which can be compared with eddy covariance estimate of total NEP. Moreover, this work may provide some useful information for future modelling of beech productivity. Our models consist of experimental relationships established at the level of the system being studied. They were intended primarily as research tools.

In this work, discrepancies observed between carbon and growth balance at tree scale were due to some uncertainties. Respiration fluxes of the aboveground biomass were not measured but estimated as the difference between ecosystem and soil respiration. Moreover, it has been shown that annual ecosystem respiration was higher than expected, probably due to dead wood decomposition on the ground of the experimental plot [25]. Chambers installed in the site will provide information about the magnitude of stem and branches respiration fluxes and distinguish construction and maintenance respiration. Improvement will be made using exponential function of soil respiration with temperature and moisture [19]. Further measurements of litterfall respiration will improve the annual budget of gas exchange.

Acknowledgements: We are grateful to Patrick Gross, Bernard Clerc and François Willm for their technical assistance during fieldwork. This research was financially supported by: 1) the European programme Euroflux (ENV4-CT95-0078) coordinated by R. Valentini (University of Tuscia, Italy), 2) the French National Forest Service (ONF), 3) a pluridisciplinary programme on interactions between Man and Environment of CNRS: “Environnement. Vie et Sociétés”. This research received funding from the Ministry of Research of the government of the Grand Duchy of Luxembourg. The authors thank E. Dreyer for helpful discussions and want to acknowledge valuable suggestions from anonymous reviewers.

REFERENCES

[1] Aber J.D., Reich P.B., Goulden M.L., Extrapolating leaf CO_2 exchange to the canopy: A generalized model of forest photosynthesis compared with measurements by eddy correlation, Oecologia 106 (1996) 257-265.

[2] Amthor J.S., The role of maintenance respiration in plant growth, Plant Cell Environ. 7 (1984) 561-569.

[3] Amthor J.S., Scaling CO_2 -photosynthesis relationships from the leaf to the canopy, Photosynthesis Research 39 (1994) 321-350.

[4] Amthor J.S., Higher plant respiration and its relationships to photosynthesis, in: Schulze E.D., Caldwell M.M. (Eds.), Ecophysiology of photosynthesis (Ecological Studies Vol. 100), Springer-Verlag, Berlin, 1994, pp. 71-101.

[5] Amthor J.S., Goulden M.L., Munger J.W., Wofsy S.C., Testing a mechanistic model of forest-canopy model mass and energy exchange using eddy covariance: Carbon dioxide and ozone uptake by a mixed oak-maple stand, Aust. J. Plant Physiol. 21 (1994) 623-651.

[6] Anderson J.M., The breakdown and decomposition of sweet chestnut (*Castanea sativa* Mill.) and beech (*Fagus sylvatica* L.) leaf litter in two deciduous woodland soils. II. Changes in the carbon, hydrogen, nitrogen and polyphenol content, Oecologia 12 (1973) 275-288.

[7] Arneth A., Kelliher F.M., Mcseveny T.M., Byers J.N., Assessment of annual carbon exchange in a water-stressed *Pinus radiata* plantation: an analysis based on eddy covariance measurements and an integrated biophysical model, Global Change Biology 5 (1998) 531-545.

[8] Baldocchi D.D., Hicks B.B., Meyers T.P., Measuring biosphere-atmosphere exchanges of biologically related gases with micrometeorological methods, Ecology 69 (1988) 1331-1340.

[9] Baldocchi D.D., Vogel C.A., Hall B., Seasonal variation of carbon dioxide exchange rates above and below jack pine forest, Agricultural and Forest Meteorology 83 (1997) 174-170.

[10] Bartelink H.H., Allometric relationships for biomass and leaf area of beech (*Fagus sylvatica* L.), Ann. Sci. For. 54 (1997) 39-50.

[11] Bréda N., Dufrêne E., Estimation of deciduous forest leaf area index using direct and indirect methods, Oecologia 104 (1995) 156-162.

[12] Bréda N., Granier A., Intra- and interannual variations of transpiration, leaf area index and radial growth of a sessile oak stand (Quercus petraea), Ann. Sci. For. 53 (1996) 521-536.

[13] Cannell M.G.R., Physiological basis of wood production: A review, Scand. J. For. Res. 4 (1989) 459-490.

[14] Ceulemans R.J., Saugier B., Photosynthesis, Physiology of Trees 2 (1991) 21-50.

[15] Denmead O.T., Transfer processes between vegetation and air: measurement, interpretation and modelling, in: Málek I., Prát S. (Eds.), Prediction and measurement of photosynthetic productivity, Pudoc, 1970, pp. 149-164.

[16] de Pury D.G.G., Farquhar G.D., Simple scaling of photosynthesis from leaves to canopies without the errors of big-leaf models, Plant, Cell and Environment 20 (5) (1997) 537-557.

[17] Dickson R.E., Tomlinson P.T., Oak growth, development and carbon metabolism in response to water stress, Ann. Sci. For. 53 (1996) 181-196.

[18] Edwards N.T., Shugart H.H. Jr., McLaughlin S.B., Harris W.F., Reichle D.E., Carbon metabolism in terrestrial ecosystems, in: Reichle D.E. (Ed.), Dynamic properties of forest ecosystems (International Biological Programme 23), Cambridge University Press, Cambridge (1980).

[19] Epron D., Farque L., Lucot E., Badot P.M., Soil CO_2 efflux in a beech forest: dependence on soil temperature and soil water content, Ann. Sci. For. 56 (1999) 221-226.

[20] Epron D., Farque L., Lucot E., Badot P.M., Soil CO_2 efflux in a beech forest: The contribution of root respiration, Ann. Sci. For. 56 (1999) 289-295.

[21] Farquhar G.D., Caemmerer S. von., Berry J.A., A biochemical model of photosynthetic CO_2 assimilation in leaves of C3 species, Planta 149 (1980) 78-90.

[22] Farquhar G.D., Sharkey TD., Stomatal conductance and photosynthesis, Ann. Rev. Plant Physiol. 33 (1982) 317-345.

[23] Gansert D., Root respiration and its importance for the carbon balance of beech saplings (*Fagus sylvatica* L.) in a montane beech forest, Plant soil. 167 (1994) 109-119.

[24] Gifford R.M., Interaction of carbon dioxide with growth-limiting environmental factors in vegetation productivity: implications for the global carbon cycle, Advances in Bioclimatology 1 (1992) 25-53.

[25] Granier A., Ceschia E., Damesin C., Dufrêne E., Epron D., Gross P., Lebaube S., Le Dantec V., Le Goff N., Lemoine D., Lucot E., Ottorini J-M., Pontailler J.Y., Saugier B., Carbon balance in a young beech forest during two years of experiment, Functional Ecology (accepted).

[26] Greco S., Baldocchi D.D., Seasonal variations of CO_2 and water vapour exchange rates over a temperate deciduous forest, Global Change Biol. 2 (1996) 183-197.

[27] Hinckley T.M., Lassoie J.P., Radial growth in conifers and deciduous trees: a comparison, Mitt Forstlichen Bundesversuchsanstalt (Vienna), 142 (1981) 17-56.

[28] Jarvis P.G., McNaughton K.C., Stomatal control of transpiration: scaling up from leaf to region, Advances in Ecological Research 15 (1986) 1-49.

[29] Kellomäki S., Oker-Blom P., Specific needle area of Scots pine and its dependence on light conditions inside the canopy, Silva Fenn 15 (1981) 190-198.

[30] Kraft G., Beitraege zur Lehre von den Durchforstubgen, Schlagstellungen und Lichtungstrieben, Klindworth, Hannover, Germany, 1884.

[31] Lachaud S., Xylogénèse chez les dicotylédones arborescentes. II. Évolution avec l'âge des modalités de la réactivation cambiale et de la xylogénèse chez le hêtre et le chêne, Can. J. Bot. 59 (1981) 2692-2697.

[32] Lachaud S., Bonnemain J.L., Xylogénèse chez les dicotylédones arborescentes. I. Modalités de la remise en activité du cambium et de la xylogénèse chez les hêtres et chênes agés, Can. J. Bot. 59 (1981) 1222-1230.

[33] Lachaud S., Bonnemain J.L., Xylogénèse chez les dicotylédones arborescentes, III. Transports de l'auxine et activité cambiale dans les jeunes tiges de hêtre, Can. J. Bot. 60 (1982) 869-876.

[34] Lang A.R.G., Leaf area and average leaf angle from transmission of direct sunlight, Aust. J. Bot. 34 (1986) 349-355.

[35] Le Goff N., Ottorini J.M., Thinning and climate effects on growth of beech (*Fagus sylvatica* L.) in experimental stands, Forest Ecology and Management 62 (1993) 1-14.

[36] Lemée G., Structure et dynamique de la hetraîe des réserves biologiques de la forêt de Fontainebleau: un cas complexe climacique de forêt feuillue monospécifique temperée, Acta Oecologica 10 (1989) 155-174.

[37] Leuning R., Kelliher F.M., De Pury D.G.G., Schulze E.D., Leaf nitrogen, photosynthesis, conductnce and transpiration: sclaing from leaves to canopies, Plant, Cell and Environment 18 (1995) 1183-1200.

[38] Malaisse F., Contribution à l'étude des hêtraies d'Europe occidentale. Note 4: Quelques observations phénologiques de hêtraies en 1963, Bull. Soc. r. Bot. Belg. 97 (1964) 85-97.

[39] Raulier F., Bernier P.Y., Ung C-H., Canopy photosynthesis of sugarmaple (*Acer saccharum*): comparing big-leaf and multilayer extrapolations of leaf-level measurements, Tree Physiology 19 (1999) 407-420.

[40] Ruimy A., Saugier B., Dedieu G., Methodology for the estimation of terrestrial net primary production from remotely sensed data, J. Geophys. Res. 99 (1994) 5263-5283.

[41] Ruimy A., Jarvis P.G., Baldocchi D.D., Saugier B., CO_2 fluxes over plant canopies and solar radiation: a review, Adv. Ecolog. Res. 26 (1996) 1-68.

[42] Ryan M.G., Slinder J.M., Vose J.M., McMurtie R.E., Dark respiration in pines, Ecol. Bull. 43 (1994) 50-63.

[43] Ryan M.G., Hubbard R.M., Pongracic S., Raison R.J., McMurtie R.E., Foliage, fine-root, woody-tissue and stand respiration in Pinus radiata in relation to nitrogen status, Tree Physiol. 16 (1996) 333-343.

[44] Santa Regina I., Tarazona T., Calvo R., Aboveground biomass in a beech forest and a Scots pine plantation in the Sierra de la Demanda area of northern Spain, Ann. Sci. For. 54 (1997) 261-269.

[45] Schimel D.S., Terrestrial ecosystems and the global carbon cycle, Global Change Biol. 1 (1995) 77-91.

[46] Sellers P.J., Berry J.A., Collatz G.J., Field C.B., Hall F.G., Canopy reflectance, photosynthesis and transpiration. III A reanalysis using improved leaf models and a new canopy integration scheme, Remote Sensing Environ. 42 (1992) 187-216.

[47] Shinano T., Osaki M., Tadano T., Problems in the methods of estimation of growth and maintenance respiration, Soil Sci. Plant Nutr. 42 (4) (1996) 773-784.

[48] Spitters C.J.T., Toussaint H.A.J.M., Goudriann J., Separating the diffuse and direct component of global radiation and its implications for modelling canopy photosynthesis. Part I. Components of incoming radiation, Agricult. Forest Meteor. 38 (1986) 225-237.

[49] Sprugel D.G., Hinckley T.M., Schaap W., The theory and practice of branch autonomy, Annu. Rev. Ecol. Syst. 22 (1991) 309-334.

[50] Valentini R., De Angelis P., Matteucci G., Monaco R., Dore S., Mugnozza G.E.S., Seasonal net carbon dioxide exchange of a beech forest with the atmosphere, Global Change Biol. 2 (1996) 199-207.

[51] Vogelmann T.C., Nishio J.N., Smith W.K., Leaves and light capture) light propagation and gradients of carbon fixation within leaves, Science 2 (1996) 65-70.

[52] Wang J., Ives N.E., Lechowicz M.J., The relation of foliar phenology to xylem embolism in trees, Funct. Ecol. 6 (1992) 469-475.

[53] Witowski J., Gas exchange of the lowest branches of young Scots pine: A cost-benefit analysis of seasonal branch carbon budget, Tree Physiol. 17 (1997) 757-765.

[54] Wofsy S.C., Goulden M.L., Munger J.W., Fan S.M., Bakwin P.S., Daube B.C., Bassow S.L., Bazzaz F.A., Net Exchange of CO_2 in a Mid-Latitude Forest, Science 260 (1993) 1314-1317.

NOTATION

A_n: net photosynthesis (μmol m^2 s^{-1})

EC: eddy covariance technique

DOY: Day Of Year

GEP_{EC}: gross assimilation calculated from eddy covariance

$$GEP_{\mathrm{EC}} = NEE - R_{\mathrm{heterotrophic}} - R_{\mathrm{autotrophic}}$$

GEP_{SL}: gross assimilation calculated from scaled leaf measurements

L/*B* ratio: leaf biomass/branch biomass ratio

LAI: Leaf Index Area (m^2 m^{-2})

NEE_{EC}: net ecosystem carbon dioxide exchange calculated from eddy covariance

NPP: net primary productivity

PAR: Photosynthetically Active Radiation (μmol m^2 s^{-1})

R_{bio}: aerial biomass respiration (μmol m^2 s^{-1})

R_{eco}: ecosystem respiration (μmol m^2 s^{-1})

$$R_{\mathrm{eco}} = R_{\mathrm{heterotrophic}} + R_{\mathrm{autotrophic}}$$

REW: Relative Extractable Water in soil

R_{ld}: leaf respiration during daylight hours

R_{root}: root respiration (μmol m^2 s^{-1})

R_{soil}: CO_2 efflux at soil surface

VPD: air Vapour Pressure Deficit.